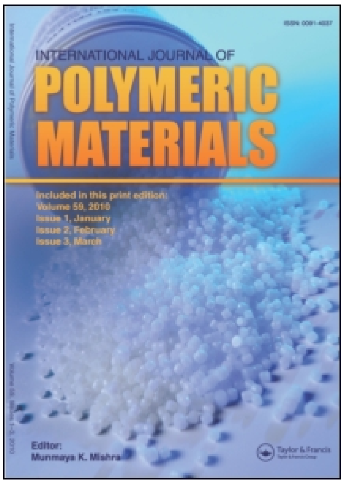

International Journal of Polymeric Materials
Publication details, including instructions for authors and subscription information:
http://www.informaworld.com/smpp/title~content=t713647664

Low Dielectric Constant Polyimide-Zirconium Nanocomposites with Improved Thermal Properties

Turgay Seçkin[a]; Süleyman Köytepe[a]; Nilüfer Kıvılcım[a]; Erkan Bahçe[b]; Ibrahim Adıgüzel[c]
[a] Department of Chemistry, Inonu University, Malatya, Turkey [b] Department of Mechanical Engineering, Malatya, Turkey [c] Department of Physics, Inonu University, Malatya, Turkey

To cite this Article Seçkin, Turgay , Köytepe, Süleyman , Kıvılcım, Nilüfer , Bahçe, Erkan and Adıgüzel, Ibrahim(2008) 'Low Dielectric Constant Polyimide-Zirconium Nanocomposites with Improved Thermal Properties', International Journal of Polymeric Materials, 57: 5, 429 — 441

To link to this Article: DOI: 10.1080/00914030701729248

URL: http://dx.doi.org/10.1080/00914030701729248

International Journal of Polymeric Materials, 57:429–441, 2008
Copyright © Taylor & Francis Group, LLC
ISSN: 0091-4037 print/1563-535X online
DOI: 10.1080/00914030701729248

Low Dielectric Constant Polyimide-Zirconium Nanocomposites with Improved Thermal Properties

Turgay Seçkin
Süleyman Köytepe
Nilüfer Kıvılcım
Department of Chemistry, Inonu University, Malatya, Turkey

Erkan Bahçe
Department of Mechanical Engineering, Malatya, Turkey

Ibrahim Adıgüzel
Department of Physics, Inonu University, Malatya, Turkey

Low-dielectric-constant (κ) polyimide films with thermal integrity and controllable mechanical strength have been prepared by covalently bonding zirconium complex with lysine to the main chains of polyimide. The presence of chemical bonds between polyimide (PI) and zirconium has great effect on the properties of polyimide films, especially on their thermal and dielectric properties. The dielectric constants of the resultant nanocomposites are lower due to the increased free volume and fewer polar Zr−O−Zr groups, and can be tuned by varying the molar ratio of zirconium(IV) propoxide, $Zr(OPr)_4$, in the feed. The possibility of obtaining the kinetic parameters of a reaction from a heating rate dependence of DTA peak location, as well as the merits of different peak methods, were also discussed. The composition, particle sizes, and morphological effect of the Zirconium on nanoparticles were determined by the energy dispersive analysis of X-ray (EDAX), and scanning electron micrographs (SEM).

Keywords: hybrid composites, nano composites, polymer matrix composite, preceramic polymer

Received 19 July 2007; in final form 27 August 2007.

The authors wish to thank the Turkish Research Council (TUBİTAK) for the research grant (105T386).

Address correspondence to Turgay Seçkin, Department of Chemistry, Inonu University, Malatya, Turkey. E-mail: tseckin@inonu.edu.tr

INTRODUCTION

The demand for low-dielectric-constant (low-κ) materials in the microelectronics industry has recently led to extensive efforts to explore the applicability of porous materials, with a special focus on ceramic materials [1–7]. Low-κ materials can be prepared by introducing voids into the film to take advantage of the low dielectric constant of air. Homogeneous, nanometer-sized, closed pores are preferred to preserve the electric and mechanical properties of the material [8–14].

Polyimides are well-known for their high-temperature durability which can exceed 400°C service temperatures, and mechanical strength. Polyimides are used as interlayer dielectrics in microelectronics applications by simple spin-coating techniques [15–30]. One approach for producing porous, low-κ polyimides is based on creating voids by thermal degradation of the polymeric block of a phase-separated polyimide—poly(propylene oxide) block copolymer [10–11]. In this approach, it is critically important to completely remove the residual organic compound and produce uniform, controllable, and closed pores [31–34].

In the present study, we implement a new approach by using organic-inorganic nanocomposites with well-defined architectures to tether Zr–O–Zr groups to the side groups of pre-synthesized polyimide to form nanoporous films. This approach can be an effective way to lower κ while maintaining certain mechanical properties of the resulting nanocomposites. Furthermore, we can have the advantage of producing materials with a tunable dielectric constant by varying the molar ratio of Zr–O–Zr in polyimide. Because accessible polymer chain ends are limited, a large number of covalently attached Zr–O–Zr pendants is needed to further reduce the dielectric constant of polyimide. The synthesis of polyimide-Zr nanocomposites is shown in Schemes 1 and 2 below.

EXPERIMENTAL SECTION

Instruments

Infrared spectra were recorded from KBr pellets in the range 4000–400 cm^{-1} on an ATI UNICAM system 2000 Fourier transform

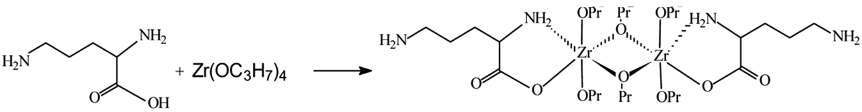

SCHEME 1 Synthesis of the zirconia dimer (Liz-Zr).

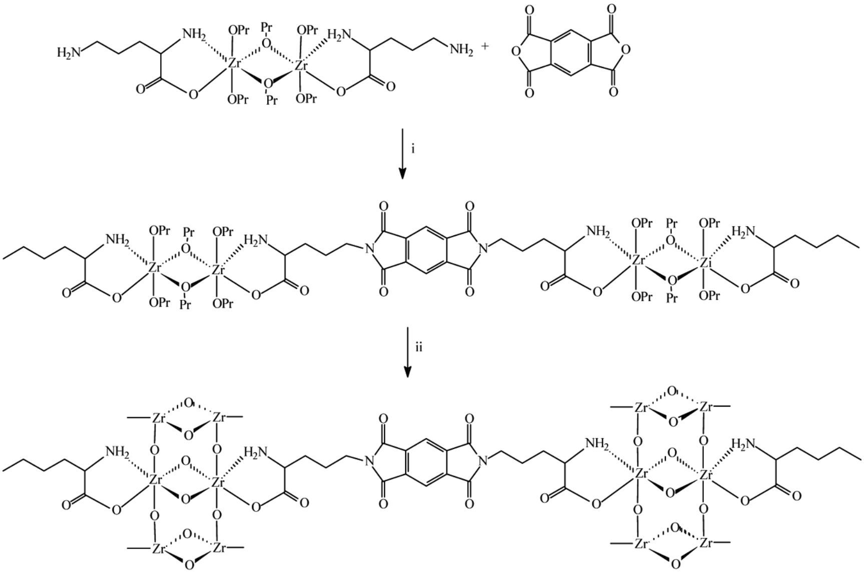

SCHEME 2 The route for the preparation of nanocomposites (Liz-PI-1 to 5).

spectrometer. ^{1}H-NMR spectra (300 MHz) and ^{13}C-NMR spectra (75.5 MHz) were obtained on a Bruker AM 300 WB FT spectrometer with δ referenced to the solvent $CDCl_3$. Elemental analyses were conducted on a Carlo Erba Elemental Analyzer, model 1106. Thermal analyses were performed with Shimadzu DSC-60, DTA-50 and TGA-50.

Chemical composition analysis by EDAX was performed with an EDAX Hitachi-S-4700 analyzer attached to a scanning electron microscope (SEM, Hitachi Ltd. S-4700). Incident electron beam energies from 3 to 30 keV had been used. In all cases, the beam was at normal incidence to the sample surface and the measurement time was 100 s. All the EDAX spectra were corrected by using the ZAF correction, which takes into account the influence of the matrix material on the obtained spectra.

Materials

All chemicals were purchased from Aldrich and used after purification. *N*-Methylpyrralidone, NMP, was distilled over CaH_2 under reduced pressure and stored over 4Å molecular sieves. Reagent grade aromatic dianhydrides were used after crystallization from the appropriate solvents. All the dianhydrides were dried under vacuum at 120°C prior to use.

Synthesis

[Zr(OPr)$_3$(lysinate)]x (Zr-Liz)

Lysine (1.46 g, 10 mmol) was added to a propanolic (50 mL) solution of Zr(OPr)$_4$ (ZrOP) (4.68 g, 10 mmol). When the suspension was heated to 60°C, the lysine dissolved. After elimination of the solvent in a vacuum, a yellowish solid was obtained. IR (Nujol) 3268 (m, NH), 1640 cm^{-1}. (vs, CO), 1614 (s), 1532 (m), 1336 (m), 1076 (m), 540 (m) cm^{-1}. Anal. Calcd for $C_{15}H_{34}N_2O_5Zr$: C, 43.6; H, 8.2; N, 6.8. Found: C, 41.9; H, 8.5; N, 6.6.

For all succeeding reactions, propanolic solutions of Zr(OR)$_3$-(lysinate) were used without subtraction of the solvent.

Hydroxyl Polyimide (PI-Zr)

Polyimide was synthesized by first racing 18.50 mmol of Zr-Liz dimer in a three-necked flask containing 90.83 g of NMP under nitrogen purge at 25°C. After the Zr-Liz dimer completely dissolved, 18.88 mmol of pyromellitic dianhydride, PMDA, were added to the flask batch-by-batch with a time interval of 0.5 h between batches. When the solids were fully dissolved in NMP, the solution was then stirred overnight under nitrogen to form the poly(amic acid) solution. The viscosity of the solution increased greatly during this period. Dry xylene (30 mL) was added to the flask, and the poly(amic acid) was imidized at 160°C for 3 h. Water that was eliminated by the ring-closure reaction was separated as a xylene azeotrope at the same time. The resultant solution was added drop-wise into an agitated solution of methanol (500 mL) and 2 N HCl (10 mL) to obtain the brown polyimide. The polymer was redissolved in NMP (50 mL) and further purified by reprecipitating into a solution of methanol (500 mL). The polymer was then filtered and dried at 60°C under vacuum for 24 h to afford 11.50 g polyimide. ‘H NMR (300 MHz, DMSO-d$_6$): 10.06 (s, 2 H, OH), 8.10 (d, 2 H, $J = 7.8$ Hz), 7.95 (d, 2H, $J = 7.8$ Hz), 7.90 (s, 2 H), 7.22 (d, 2H, J = 7.8 Hz), 7.18 (s, 2 H), 7.14 ppm (d, 2 H). Molecular weight: M_w (74000, M_n) 36000, with a polydispersity of 2.05.

Polyimide-Side-Chain Tethered Zirconium (Liz-PI-1 to 5)

Polyimide (PI-Zr) (2.00 g) was dissolved in NMP and THF (15:15 mL) at room temperature. After the mixture was stirred for 1 h, various amounts of zirconium(IV) isopropoxide were added and the solution then heated to 80°C for 3 h. The feed molar ratios of zirconium(IV) isopropoxide with respect to the equivalent of phenyl hydroxyl of polyimide were 10, 20, and 40 mol%. After filtration, the reaction mixture was slowly added to excess H_2O. The resultant powder was washed with MeOH and then dried in an oven.

Zirconium-polyimide nanocomposite films were prepared by dissolving the nanocomposite powder (1.00 g) in NMP/THF cosolvent (5 mL/5 mL) and casting it on glass slides with a doctor blade, followed by drying in vacuum at 50°C for 24 h and then at 200°C for 12 h. The resulting films were then peeled off the glass slides as self-standing films for all thermal evaluations.

RESULTS AND DISCUSSION

The preparation of polyimides is summarized in Scheme 2. The intermediates and polymers were characterized by ^{13}C NMR, elemental analysis, and FTIR spectra. Scheme 2 shows that lysine substitution was successful in every case. The two zirconium atoms in the starting cluster are capped by one oxygen atom and one alkoxy group. There are two bridging ethoxy groups around the edges of the triangle, and the remaining ethoxy groups are terminally bonded. Substitution of a carboxylate group for the first alkoxy group is according to the rules: a bridging alkoxy group, that is a bidendate group with a single negative charge, is substituted by another bidentate group with a single negative charge. This means that one of the coordination sites at one of the zirconium atoms must be left empty. In this case, the zirconium cluster is quite tolerant. X-ray analysis of Liz-Zr showed the compound to be dimeric with two bridging propoxy groups. The data we obtained is consistent with the data given by Schubert et al. [11]

The results are in agreement with the proposed structures. Thus, the FTIR spectra of all polyimides showed distinct features that clearly indicate imide ring formation and the disappearance of the polyamic acid peak during the thermal cyclization step. The characteristic absorption bands of amic acid and carboxyl groups in the 3240 to 3320 cm^{-1} and 1500 to 1730 cm^{-1} regions disappear and those of the imide ring appear near 1770 cm^{-1} (asym. C=O stretching) and 1720 cm^{-1} (sym. C=O stretching), 1373 cm^{-1} (C–N stretching) 1053 cm^{-1} and 723 cm^{-1} imide (ring deformation).

Figure 1a shows the infrared spectrum of the ZrO_2 precursors obtained from the first step of Scheme 2. The broad absorption band below 1000 cm^{-1} corresponds to ν (Zr–O–Zr) vibrations. This shows that –Zr–O–Zr– networks are formed. The two intense bands around 1440 and 1550 cm^{-1} can be respectively assigned to the symmetric and antisymmetric stretching vibrations of carboxylate groups, $\nu_s(COO^-)$ and $\nu_{as}(COO^-)$. Their position and frequency splitting ($\Delta\nu = 110\,cm^{-1}$) indicated that the carboxylate groups of lysine

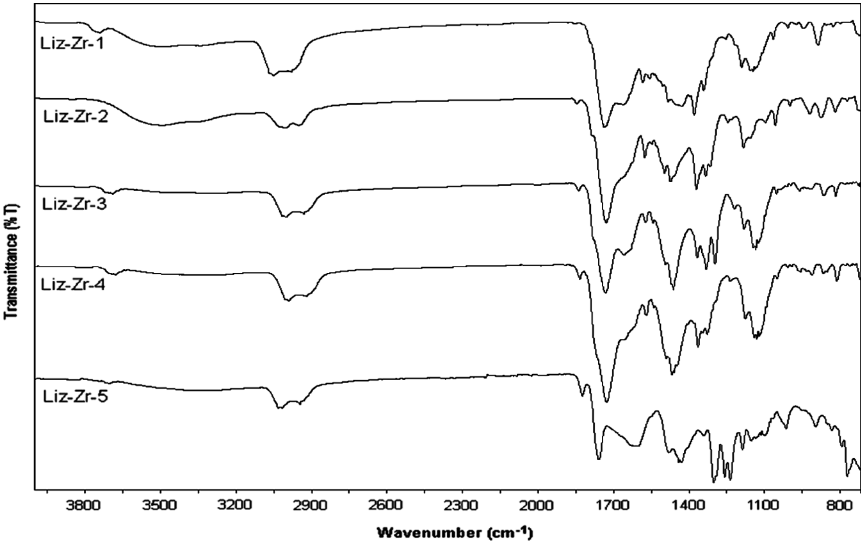

FIGURE 1 FT-IR spectra of nanocomposites Liz-PI-1 to 5.

molecules were bound to zirconium atoms in a chelating bidentate configuration.

The chemical modification decreased the hydrolytic susceptibility of $Zr(OPr)_4$ and promoted decoupling between hydrolysis and condensation reactions, allowing the formation of the dispersible ZrO_2 precursors. The infrared spectrum of the nanomaterials was similar to Figure 1 with the characteristic features of chelating carboxylate groups ($\nu_s(COO^-) = 1450\,cm^{-1}$, $\upsilon_{as}(COO^-) = 1540\,cm^{-1}$, and $\Delta\upsilon = 90\,cm^{-1}$) and those of alkyl groups (δ (C–H) $\sim 1300\,cm^{-1}$ and $\nu(C{-}H) = 2820–3020\,cm^{-1}$), indicating the chelation of lysine molecules onto the ZrO_2 surfaces. Zirconium-doped Liz-Zr-PAA poly(amic acid) solutions were prepared by first dissolving the Liz-Zr complex in N-methyl-2-pyrollidone (NMP), and then adding a THF solution of the poly(amic acid) to give a 15 wt% polymer (excluding the complex) solution. The polymer-to-complex mole ratio was calculated in order to obtain a theoretical weight percent of Zr; i.e., 13% in the final polyimide film, which represents 1.97% volume percent. These values were calculated on the basis of only Zr-polyimide remaining in the cured films. The clear complex-doped resins were cast as films onto soda lime glass plates using a doctor blade set to give cured films with ca. 40 μm thickness. After remaining in an atmosphere of slowly flowing dry air for 12–18 h, the films were cured in the following

TABLE 1 Preparation and Thermal Properties of Polyimide/Zirconium Hybrid Films

Entry	ZrOP (g)	DMAc (g)	Zr[a] (wt%)	Ash[b] (wt%)	T_d[c] (°C)
1	0	4.12	0	–	506
2	0	4.12	~0	0.92	505
Liz-PI-1	0.36	4.12	5	2.0	550
Liz-PI-2	0.77	4.12	10	5.4	544
Liz-PI-3	1.22	4.12	15	9.8	565
Liz-PI-4	1.73	4.12	20	14.5	562
Liz-PI-5	2.97	4.12	30	24.4	598

[a] Calculated zirconia content in the hybrid films.

[b] Residual ash from TGA results.

[c] T_d: 5 wt% decomposition temperature. Deionized water, drying, and storing under atmospheric conditions until measurements were performed.

manner: heating to 135°C for 20 min and holding at that temperature for 1 h, then heating to 300°C over 4 h and holding at 300°C for 1 h.

FT-IR Spectra of Nanocomposites Liz-PI-1 to 5

The zirconium oxide (ZrO_2) content in Table 1 denotes the values calculated by assuming the sol-gel reaction proceeded to completion. All the solutions of the precursor polymeric mixture before casting were homogeneous. The polyimide-zirconium hybrid films were obtained as self-standing yellow films even after curing at 300°C. The films became opaque when the zirconium content was more than 30 wt%. The residual ash from TG analysis is lower than the calculated zirconium content. The reasons for this are that the hydrolysis reaction proceeded very slowly because of the additional water coming from the reaction itself, and some of unreacted Liz-Zr was removed from the reaction system and due to the fact that PAA is a weak acid to the zirconium system compared to a strong acid such as HCl.

The thermal properties of the monomer and all polyimides were evaluated by thermogravimetry (TG), differential thermal analysis (DTA) and differential scanning calorimetry (DSC). The results are summarized in Table 2. Depending on the structure of the dianhydride components, which affect the stiffness of the polymer backbones, the Tg values of the polyimides (Liz-PI-1 to Liz-PI-5) were in the range of 150–193°C. The temperatures for 10% weight loss (under nitrogen), char yield, and initial decomposition temperature were determined from the original thermograms (Table 2). The 10% weight loss temperatures (Figures 2 and 3) for the polymers were between 405 and 423°C.

TABLE 2 Thermal Properties of Nanocomposites (Liz-PI-1 to 5)

Polymer	Liz-PI-5	Liz-PI-4	Liz-PI-3	Liz-PI-2	Liz-PI-1
TGA Analysis					
On set	387	392	381	331	317
End set	632	625	618	591	588
% 10[a]	419	423	411	405	415
IDT[b]	385	389	380	323	308
DTA Analysis[c]					
On set	343	346	347	329	371
End set	458	482	466	461	447
Heat (J/g)	461	716	287	165	183
TDP[d]	497	513	500	504	498
On set	458	482	466	461	447
End set	623	635	600	596	573
Heat (kJ/g)	0.90	1.14	1.46	1.57	1.46
DSC Analysis					
On set	170	134	190	160	132
End set	188	139	195	187	168
Transition (mW)	−1.87	−0.45	−0.72	−0.61	−1.99
Tg (°C)[e]	193	182	181	167	150

[a] Temperature of 10% weight loss was assessed by TGA at a heating rate of 10°C/min in N_2.

[b] IDT (initial decomposition temperature) is the temperature at which an initial loss of mass was observed.

[c] DTA thermograms of polyimides with a heating rate of 10°C/min in a air atmosphere.

[d] TDP (thermal decomposition peak).

[e] Determined by DSC in N_2 atmosphere.

The Liz-PI-1 and Liz-PI-2 had a relatively high thermal decomposition temperature because of its rigid structure. The char yields, which included two distinct groups, were over 30% in all cases; the first group with a rigid structure was in the range 50–52%. The TG analysis (Figure 3) under nitrogen showed no significant weight loss below 317°C. The initial decomposition temperature (IDT) for most of the polymers lies between 308 and 385°C. The thermal properties of the polyimide-zirconium films, the decomposition temperature (T_d) for the 5 wt % material (Liz-PI-1), and residual ash are summarized in Table 2.

TG curves do not show a weight loss below 100°C, indicating no water or propanol remained in the films. It is generally believed that the introduction of inorganic components into organic materials can improve their thermal stability since inorganic elements generally have good thermal stability. However, because of the possible reaction

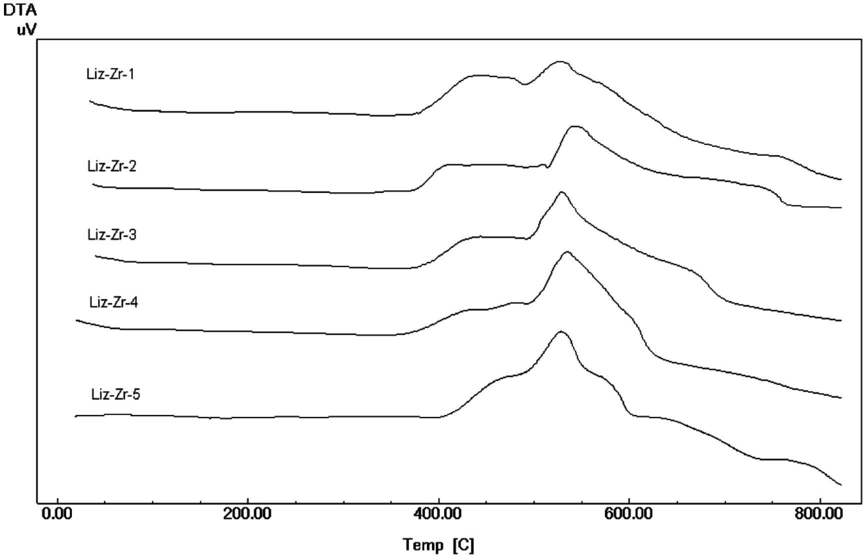

FIGURE 2 DTA curves of nanocomposites Liz-PI-1 to 5.

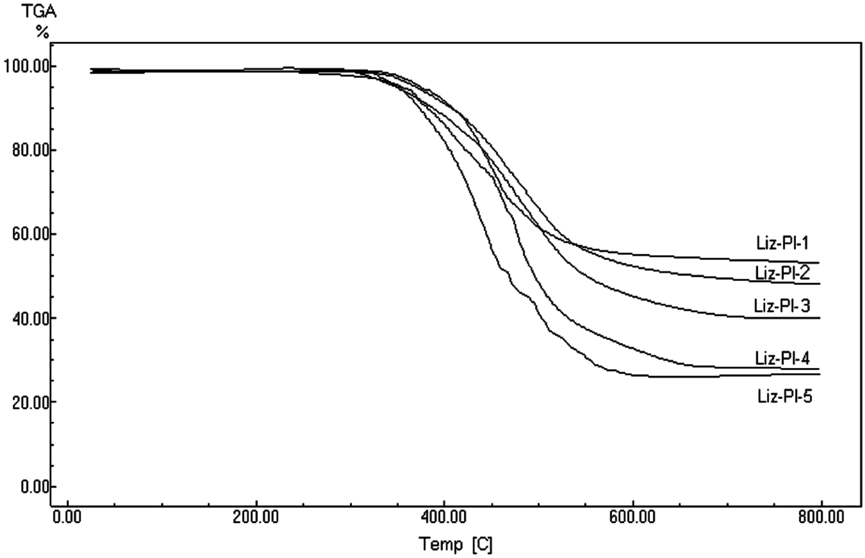

FIGURE 3 TGA curves of nanocomposites Liz-PI-1 to 5.

between them and the polymer precursor at high temperature, the cyclization of polyamic acid to form polyimide may not be complete, and this could reduce the thermal stability of the polyimide. The results (Table 2) for these hybrid films show no apparent decrease in thermal decomposition temperature. The 5 wt% loss occurred at

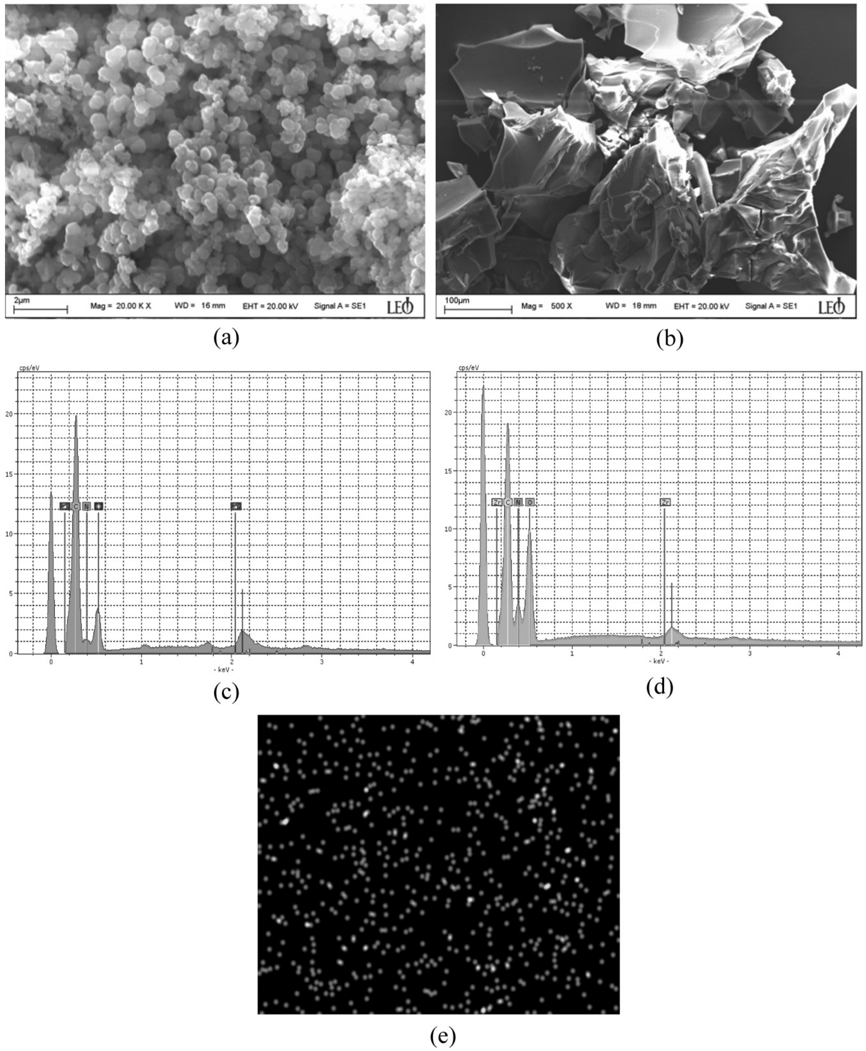

(a) (b) (c) (d) (e)

FIGURE 4 SEM micrographs and EDAX spectra of the dimer (a)–(c) and the nanocomposite (Liz-PI-1) (b)–(d), e) SEM-EDAX mapping of zirconium in the nanocomposite (Liz-PI-1).

around 500°C. The weight residue remaining at 800°C is regarded as the true zirconium content as ZrO_2 (see Table 1, column 5).

The DSC analysis was used to determine the glass transition temperature of the different nanocomposites and neat polyimide films (Table 2). No great differences in T_g values are observed between the zirconium-based polyimide-hybrids. Hence, it seems that little or no variation in chain mobility near the nanoparticle's surface is observed.

Figure 4 illustrates the nanocomposite powders as studied from the SEM investigations. One can notice that fine precipitates are formed of spherical-like particles of mean diameter particle size about 200 nm, the uniform sphere particles with diameters of 120–165 nm were obtained as shown in Figure 4a. The morphology of the products has been shown in Figure 4b. It shows that the quantity of zirconium oxide has an important effect on the morphologies of the products. From the EDAX point analysis illustrated in Figures 4c and 4d, the zirconium content of the investigated material was 2.4 wt% of the total composite content.

The dielectric constant of the Zr-polyimide nanocomposites decreases, and the relative porosity increases as the amount of ZrOP

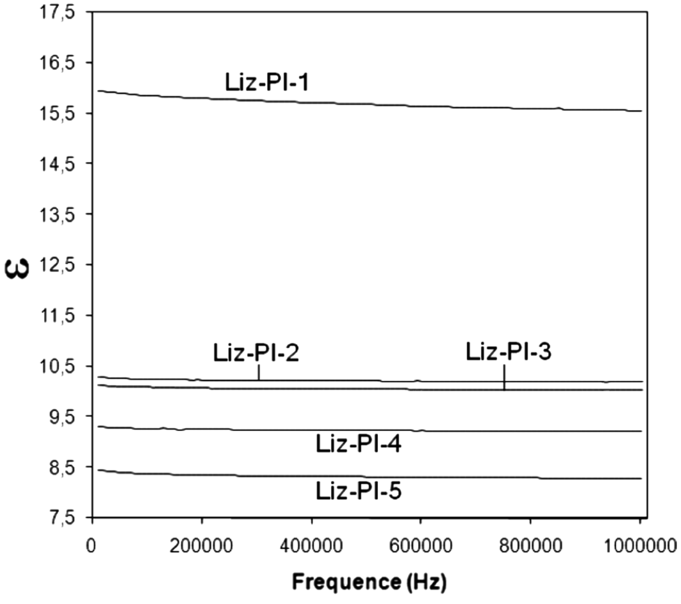

FIGURE 5 Dielectric constant (ε) of nanocomposites Liz-PI-1 to 5 at room temperature in the frequency range 20–1000 MHz.

increases (Figure 5). There are several possible reasons for the reduction in the dielectric constant. Since the porosities of the nanocomposite films are difficult to determine we adopted a simple measure to compare the relative porosities of these films. Consequently, the reduction is most likely due to the nanoporosity in the core of the ZrOP groups and the peripheral porosity introduced by tethering Zr–O–Zr to the polyimide side chains, as evidenced by the decreasing density and the increasing relative free volume of the nanocomposite films.

The increase in the external porosity in the nanocomposites is a result of ZrOP. This can be further interpreted as an increase in the free volume of the nanocomposites on account of the interaction of polyimide segments and ZrOP. This also means that the free volume of the polyimide in the nanocomposites increases with the amount of the ZrOP. The free volume of polyimide corresponds quite well to the fact that the glass transition temperature (T_g) of the polyimide in the nanocomposites is lower than that of the pure polyimide. Another possible input to the lower dielectric constant comes from the fact that the hydroxyl groups on polyimide are partly replaced by ZrOP groups.

CONCLUSIONS

The modification of zirconium alkoxides with lysine results in a derivative with cation-coordinating capability which can be employed for the preparation of zirconate materials which can bind additional metal ions. Hybrid films were obtained by the hydrolysis-polycondensation of propoxy groups (in the monomer and polymer backbone) at 200°C. The dielectric constant of the pure polyimide and polyimide/zirconia hybrid composite films with dissimilar ZrOP contents differ when an essential amount of ZrOP was introduced into PI. The dielectric constant was remarkably reduced but was found to be increased with further increasing ZrOP content. However, the value of a polyimide containing 30 wt% of Zr is still lower than that of the pure polyimide. This may be explained as due to the increasing free volume and domain sizes of ZrOP. Higher ZrOP content can cause the appearance of larger domains, made of three-dimensional networks, that bond PI blocks together, and bigger ZrOP domains from higher amount of the ZrOP contents together, they may increase the separation between the PI interblock and increase the free volume. Usually, free volume is easily occupied by moisture and increases the dielectric constant because of the inherently high dielectric constant of polyimide. It may be assumed that the Zr–O–Zr and the Zr–O bond in the cured network structure can also lead to increase dielectric constant with increasing content of the ZrOP.

REFERENCES

[1] Baskaran, S., Liu, J., Domansky, K., Kohler, N., Li, X. H., Coyle, C., Fryxell, G. E., Thevuthasan, S., and Williford, R. E., *Adv. Mater*. **12**, 291 (2000).

[2] Schubert, U., Trimmel, G., Moraru, B., Tesch, W., Fratzl, P., Gross, S., Kickelbick, G., and Hüsing, N., *Mat. Res. Soc. Symp. Proc*. **CC2.3.1**, 628 (2001).

[3] (a) Trimmel, G., Fratzl, P., and Schubert, U., *Chem. Mater*. **12**, 602 (2000); (b) Schubert, U., Völkel, T., and Moszner, N., *Chem. Mater*. **13**, 3811 (2001).

[4] Chen, H., Xie, L., Lu, H., Yang, Y., *J. Mater. Chem*. **17**, 1258 (2007).

[5] Kresge, C. T., Leonowicz, M. E., Roth, W. J., and Vartuli, J. C., *Nature* **359**, 710 (1992).

[6] Feger, C. and Franke, H. (1996). In *Polyimides Fundamentals and Applications*. M. K. Ghosh and K. L. Mittal, Eds., Marcel Dekker, New York, p. 7.

[7] Leu, C. M., Wu, Z. W., and Wei, K. H., *Chem. Mater*. **14**, 3016 (2002).

[8] Jiang, L. Y., Leu, C. M., and Wei, K. H., *Adv. Mater*. **14**, 426 (2002).

[9] Carter, K. R., Dipietro, R. A., Sanchez, M. I., Russell, T. P., Lakshmanan, P., and McGrath, J. E., *Chem. Mater*. **9**, 105 (1997).

[10] Carter, K. R., DiPietro, R. A., and Sanchez, M. I., *Chem. Mater*. **13**, 213 (2001).

[11] Schubert, U., Tewinkel, S., and Lamber, R., *Chem. Mater*. **8**, 2047 (1996).

[12] Haddad, T. S., Viers, B. D., and Phillips, S. H., *Journal of Inorganic and Organometallic Polymers* **11**, 155 (2001).

[13] Gilman, J. W., Schlitzere, D. S., and Lichtenhan, J. D., *J. Appl. Poly. Sci*. **60**, 591 (1996).

[14] Gonzalez, R. I., Phillips, S. H., and Hoflund, G. B., *J. Space, Rockets* **37**, 463 (2000).

[15] Laine, R. M., Choi, J., and Lee, I., *Adv. Mater*. **13**, 800 (2001).

[16] Zhang, C. and Laine, R. M., *J. Am. Chem. Soc*. **122**, 6979 (2000).

[17] Tamaki, R., Tanaka, Y., Asuncion, M. Z., Choi, J., Laine, R. M., *J. Am. Chem. Soc*. **123**, 12416 (2001).

[18] Zheng, L., Waddon, A. J., Farris, R. J., and Coughlin, E. B., *Macromol*. **35**, 2375 (2002).

[19] Zhang, C., Babonneau, F., Bonhomme, C., Laine, R. M., Soles, C. L., Hristov, H. A., and Yee, A. F., *J. Am. Chem. Soc*. **120**, 8380 (1998).

[20] Lichtenhan, J. D., Vu, N. Q., Carter, J. A., and Gilman, J. W., *Macromol*. **26**, 2141 (1993).

[21] Lichtenhan, J. D., Otonari, Y. A., and Carr, M. J., *Macromolecules* **28**, 8435 (1995).

[22] Haddad, T. S. and Lichtenhan, J. D., *Macromolecules* **29**, 7302 (1996).

[23] Lee, A. and Lichtenhan, J. D., *Macromolecules* **31**, 4970 (1998).

[24] Feher, F. J., Soulivong, D., and Eklud, A. G., *Chem. Commun*., 1185 (1997).

[25] Fu, B. X., Zhang, W. H., Hsiao, B. S., Rafailovich, M., Sokolov, J., Sauer, B. B., Phillips, S., and Blanski, R., *High Perform. Polym*. **12**, 565 (2000).

[26] Schmidt, H., *J. Non-Cryst. Solids* **73**, 681 (1985).

[27] Gross, S., Noto, V. D., and Schubert, U., *J. Non-Cryst. Solids* **322**, 154 (2003).

[28] Wen, J. and Mark, J. E., *Polym. J*. **27**, 492 (1995).

[29] Clarson, S. J. and Mark, J. E., *Polym. Commun*. **28**, 249 (1987).

[30] Novak, B. M., Auerbach, D., and Verrier, C., *Chem. Mater*. **6**, 282 (1994).

[31] (a) Judeinstein, P., *Chem. Mater*. **4**, 4 (1992); *Chem Euro J*., **6**, 105 (2000); (b) Mayer, C. R., Fournier, R., and Thouvenot, R., *Chem. Eur. J*., 6 (2000).

[32] Judenstein, P. and Schmidt, H., *J. Sol-Gel Sci. Techn*. **3**, 189 (1994).

[33] Mayer, C. R., Thouvenot, R., and Lalot, T., *Chem. Mater*. **12**, 257 (2000).

[34] Mijatovic, I., Kickelbick, G., and Schubert, U., *Europ. J. Chem*., 1933 (2001).